

Supplemental Experimental Procedures

Glacial meltwater samples

Field Collections

Samples were isolated by filtering 15-30L on 0.22 μm filters at the field site. All samples had high loads of glacial sediments ($\sim 0.3\text{-}1\ \mu\text{m}$). One quarter of each filter was set aside for DNA extraction and the remaining filter portions were used to isolate bacteria from the glacial sediments for proteomics.

DNA Samples: preparation and analysis

PowerSoil extraction kits from QIAGEN were used and the provided protocol was followed. We isolated $>2.5\ \mu\text{g}$ of DNA from each sample to complete the metagenome using Illumina NextSeq sequencing. Samples were submitted to the Northwest Genome Sequencing Center (University of Washington) for library preparation, and sequencing using NextSeq at 150 base pair – paired end reads (PE150). Each sample was barcoded and all 5 were loaded onto 1 lane. Trimming, filtering and assembly were completed following Timmins-Schiffman (1). The metagenome FASTA files for subsurface early melt, subsurface late melt, subsurface midseason melt, surface early melt, and surface midseason melt had 74817, 39151, 86946, 71401, and 36681 entries, respectively.

Protein Samples: preparation and analysis

In order to isolate the bacterial cells from the glacial sediments on the filters, we modified a protocol published by Kallmeyer et al. (2) to be more amenable to mass spectrometry and the low bacterial cell counts found at these sites. Emulsifier mixture included 100 mM EDTA and 100 mM sodium pyrophosphate (4°C). Additionally, bacterial cell buffer (BCB) was made to stabilize cells during the isolation procedure (4 mL of phosphate buffered saline, 645 μl emulsifier mixture, 516 μl of methanol; 4°C). To kill the samples prior to sample preparation, as it is a very lengthy process, 5 g of the sediment-bacteria mixture was rinsed with 1 ml of 0.1% sodium azide in 1 x phosphate buffered saline (PBS). Samples were vortexed and then iced 5 times (2 minutes per cycle). Bacteria and sediments were pelleted by centrifugation (10,000 x g, 4°C, 2 hours) and supernatant was removed. The sediment pellet was resuspended in 5 ml of 4°C BCB, vortexed and then iced 5 times (2 minutes per cycle) until a smooth solution was achieved. Centrifuge tubes were then placed in an ice water bath that had a Bronson sonicating probe inserted into the water (10 min; power 5). The resulting sediment slurry was then divided among 6 different 5mL ultracentrifuge tubes ($\sim 1\text{ml}$ of sediment slurry per tube). Using a syringe, 3.5mL of 40% (w/v) Nycodenz solution was injected beneath the slurry to make the sediment “float” on top of the Nycodenz. Samples were ultracentrifuged for 18 hours (50,000 x g, 4°C; Beckman SW50.1 rotor; no deceleration brake). The overlying clear layer contains the bacterial fraction and was collected with needle and syringe, pooled and 60 mL 1x PBS was added to decrease the density of the Nycodenz solution. This allowed us to isolate the bacterial cells using ultracentrifugation. Samples were then centrifuged for 15 hours (10,000 x g, 8°C) and the overlying liquid was removed carefully as to not disturb the cell pellets. Cell pellets were combined for each sample to

yield one final cell pellet. These were rinsed and pelleted 3x with 500ul of 50 mM ABC. Cell pellets were digested with 1 µg of trypsin each following Nunn et al. (3).

Samples were analyzed on the Q-Exactive in DDA mode using an inline chromatography system (Waters Nanoacquity) with a 4cm precolumn (100um ID) and 30cm PicoTip analytical column (75um ID) maintained at 50°C (Dr. Maisch C18). Peptides were separated with a 120-minute gradient from 2% -35% acetonitrile, 0.1% formic acid, with total runtime of 160 minutes. Total ion current per sample was ~5E9 per injection. MS and MS/MS scans were collected at 70,000 and 35,000 resolution, respectively, using a loop count of 20 per DDA cycle with a dynamic exclusion of 10 sec and exclusion of all +1, >+5 ions.

References

1. Timmins-Schiffman, E., May, D. H., Mikan, M., Riffle, M., Frazar, C., Harvey, H. R., Noble, W. S., and Nunn, B. L. (2017) Critical decisions in metaproteomics: Achieving high confidence protein annotations in a sea of unknowns. *ISME J.* 11, 309–314
2. Kallmeyer, J., Smith, D. C., Spivack, A. J., and D'Hondt, S. (2008) New cell extraction procedure applied to deep subsurface sediments. *Limnol. Oceanogr. Methods* 6, 236–245
3. Nunn, B. L., Slattery, K. V., Cameron, K. A., Timmins-Schiffman, E., and Junge, K. (2015) Proteomics of *Colwellia psychrerythraea* at subzero temperatures - a life with limited movement, flexible membranes and vital DNA repair. *Environ. Microbiol.* 17, 2319–2335

Supplemental Tables

Table S1: Novor results for high mass accuracy fragment ion MS/MS spectra using an orbitrap. A tryptic digest of a human cell line was subjected to either beam CID or resonance CID. Database searches with FDR < 0.001 and Comet E-value < 0.001 gave 16,062 (beam CID) and 14,344 (resonance CID) PSMs. Recall values and the Novor sequence score for a few precision values are shown, along with the number of *de novo* sequences with an equal or greater score. Sequencing rate is the number of correct *de novo* sequences for a given precision divided by the total number of spectra.

Precision	Recall	Novor score	# <i>de novo</i> sequences	Sequencing rate (%)
Beam CID 16,062 spectra total				
0.99	0.64	74	8,395	52.3
0.98	0.77	67	10,204	63.5
0.95	0.91	58	12,342	76.8
0.90	0.98	46	14,037	87.4
0.85	0.99	30	15,171	94.5
Resonance CID 14,344 spectra total				
0.99	0.74	59	7,654	53.4
0.98	0.79	55	8,310	57.9
0.95	0.86	50	9,372	65.3
0.90	0.94	42	10,778	75.1
0.85	0.98	35	11,868	82.7

Table S2: Novor results for low mass accuracy fragment ion MS/MS spectra using a linear ion trap. A tryptic digest of a human cell line was subjected to either beam CID or resonance CID. Database searches with FDR < 0.001 and Comet E-value < 0.001 gave 9,303 (beam CID) and 11,082 (resonance CID) PSMs. Recall values and the Novor sequence score for a few precision values are shown, along with the number of *de novo* sequences with an equal or greater score. Sequencing rate is the number of correct *de novo* sequences for a given precision divided by the total number of spectra.

Precision	Recall	Novor score	# <i>de novo</i> sequences	Sequencing rate (%)
Beam CID 9,303 spectra total				
0.99	0.15	85	633	6.8
0.98	0.26	81	1,067	11.5
0.95	0.37	78	1,575	16.9
0.90	0.54	72	2,452	26.4
0.85	0.68	68	3,245	34.9
Resonance CID 11,082 spectra total				
0.99	0.48	82	3,278	29.6
0.98	0.62	78	4,307	38.9
0.95	0.79	70	5,637	50.9
0.90	0.87	64	6,535	59.0
0.85	0.92	60	7,309	66.0

Table S3: Effect of bad data on ability of Novor to assign *de novo* sequences. Starting with a human tryptic digest LCMSMS data file, ion m/z values were randomized (adding or subtracting the integers 1 to 9) to varying extents, and the number of unique *de novo* sequences with sequence scores ≥ 60 were counted.

Fraction of randomized fragments	# Unique sequences
0%	20,453
5%	17,485
10%	13,351
25%	4,084
50%	322

Table S4: Novor results summary for glacial melt water proteomics. Automated *de novo* sequencing by Novor (sequence score cutoff of 60) shows that 20-25% of the MS/MS spectra were high quality peptide spectra.

Sample	Total ms2	Total high scoring <i>de novo</i> sequences	% ms2 spectra with high scoring <i>de novo</i> sequences	# unique <i>de novo</i> sequences
Early season, surface melt	23,261	4,432	19.1%	3,715
Early season, subsurface melt	22,249	4,207	18.9%	3,437
Mid season, surface melt	21,879	5,443	24.9%	4,347
Mid season, subsurface melt	22,292	5,919	26.6%	4,521
Late season, subsurface melt	18,873	4,494	23.8%	3,246

Table S5: An example where the correct FASTA-derived sequence is ranked below a *de novo* sequence. The difference in the order of the two N-terminal amino acids was sufficient to give the *de novo* sequence a slightly higher cross-correlation score.

Rank	Sequence	Xcorr	FASTA / de novo
1	KSEEAELYHSK	4.351	De novo
2	SKEEAELYHSK	4.108	FASTA
3	SHYLAEEKSK	0.960	FASTA

Table S6: Human LCMSMS data searched against FASTA files of various other species to which high scoring (≥ 60) *de novo* sequences had been appended. The column “Database unique (%)” is plotted in Fig. 4.

Species	Common name	Taxonomy (phylum/class/order/family)	Total PSMs	Total unique sequences	Novor PSMs	Novor unique sequences	Database PSMs (%)	Database unique sequences (%)
H. sapiens	human	Chordata/mammalia/primate/hominidae	35,488	19,693	2,937	1,804	91.7	90.8
H.sapiens, shuffled	Randomized human		24,800	13,793	24,732	13,737	0.3	0.4
P. troglodytes	chimp	Chordata/mammalia/primate/hominidae	34,636	19,142	3,679	2,284	89.4	88.1
G. gorilla	gorilla	Chordata/mammalia/primate/hominidae	34,198	18,902	4,555	2,734	86.7	85.5
P. abelii	orangutan	Chordata/mammalia/primate/hominidae	33,659	18,555	5,086	3,147	84.9	83.0
O. garnettii	galago	Chordata/mammalia/primate/galagidae	30,676	16,769	9,614	5,622	68.7	66.5
F. catus	cat	Chordata/mammalia/carnivora/felidae	30,935	16,844	8,993	5,404	70.9	67.9
S. harrisi	Tasmanian devil	Chordata/mammalia/dasyuromorphia/dasyuridae	28,709	15,639	13,597	7,942	52.6	49.2
O. anatinus	platypus	Chordata/mammalia/monotremata/ornithorhynchidae	28,090	15,345	15,850	9,195	43.6	40.1
C. brachyrhynchos	crow	Chordata/aves/passeriformes/corvidae	27,735	15,155	17,508	10,119	36.9	33.2
X. laevis	frog	Chordata/amphibian/anura/pipidae	26,370	14,402	17,061	9,766	35.3	32.2
G. aculeatus	fish (stickleback)	Chordata/actinopterygii/gasterosteiformes/gasterosteidae	26,288	14,486	19,502	11,061	25.8	23.6
B. floridae	lancelet	Chordata/leptocardii/amphioxiformes/branchiostomidae	25,356	13,985	22,653	12,753	10.7	8.8
T. Asiatica	tape worm		25,859	14,342	24,445	13,764	5.6	4.0

Table S7: *C. elegans* LCMSMS data searched against FASTA files of various other nematode species to which high scoring (≥ 60) *de novo* sequences had been appended. The column “Database unique (%)” is plotted in Fig. S3.

Species	Common name	Taxonomy (phylum/class/order/family)	Total PSMs	Total unique sequences	Novor PSMs	Novor unique sequences	Database PSMs (%)	Database unique sequences (%)
<i>C. elegans</i>	<i>C. elegans</i>	Nematoda/Chromadorea/Rhabditida/Rhabditoidea	25,273	13,888	2825	1,568	88.8	88.7
<i>C. elegans</i> , shuffled	<i>C. elegans</i>		18,933	10,420	18,906	10,395	0.1	0.2
<i>C. briggsae</i>	Most related to <i>C. elegans</i>	Nematoda/Chromadorea/Rhabditida/Rhabditoidea	21,324	11,610	10,456	5,855	51.0	49.6
<i>N. americanus</i>	Human hookworm	nematoda/chromadorea/rhabditida/Ancylostomatidae	20,048	10,892	16,335	9,009	18.5	17.3
<i>D. viviparus</i>	Lung worm	Nematoda/chromadorea/Rhabditida/Dictyocaulidae	20,109	10,956	16,713	9,238	16.9	15.7
<i>O. dentatum</i>	Nodular worm	Nematoda/chromadorea/rhabditida/cloaciniidae	19,843	10,827	16,634	9,188	16.2	15.1
<i>H. bacteriophora</i>	Entomopathogenic nematode	nematoda/chromadorea/rhabditida/heterorhabditidae	19,903	10,896	18,090	9,976	9.1	8.4

Supplemental Figures

Figure S1: Modeling molecular weight normalized cross-correlation scores using first and second ranked decoy matches. Correct database hits can sometimes have slightly lower xcorr scores than nearly correct *de novo* sequences due to incidental matching of an extra fragment ion or two (e.g., Table S5). Likewise, the top decoy sequence matches an extra fragment ion or two compared to the second best decoy sequence. Here we show the molecular weight normalized xcorr score differences between slightly incorrect *de novo* sequences and correct but lower scoring database sequences (orange), compared to score differences between first and second ranked decoy hits (blue). The left panel shows results from a human tryptic digest, and the right panel shows results from a *C. elegans* tryptic digest. These results suggest that the decoy xcorr values provide a useful model for determining score cutoffs for deciding when a second ranked database sequence has a sufficiently close xcorr value to be considered correct. In these data a molecular weight normalized xcorr score difference of 0.0002 would capture about 95% of the cases where a correct database sequence is ranked second after a *de novo* sequence.

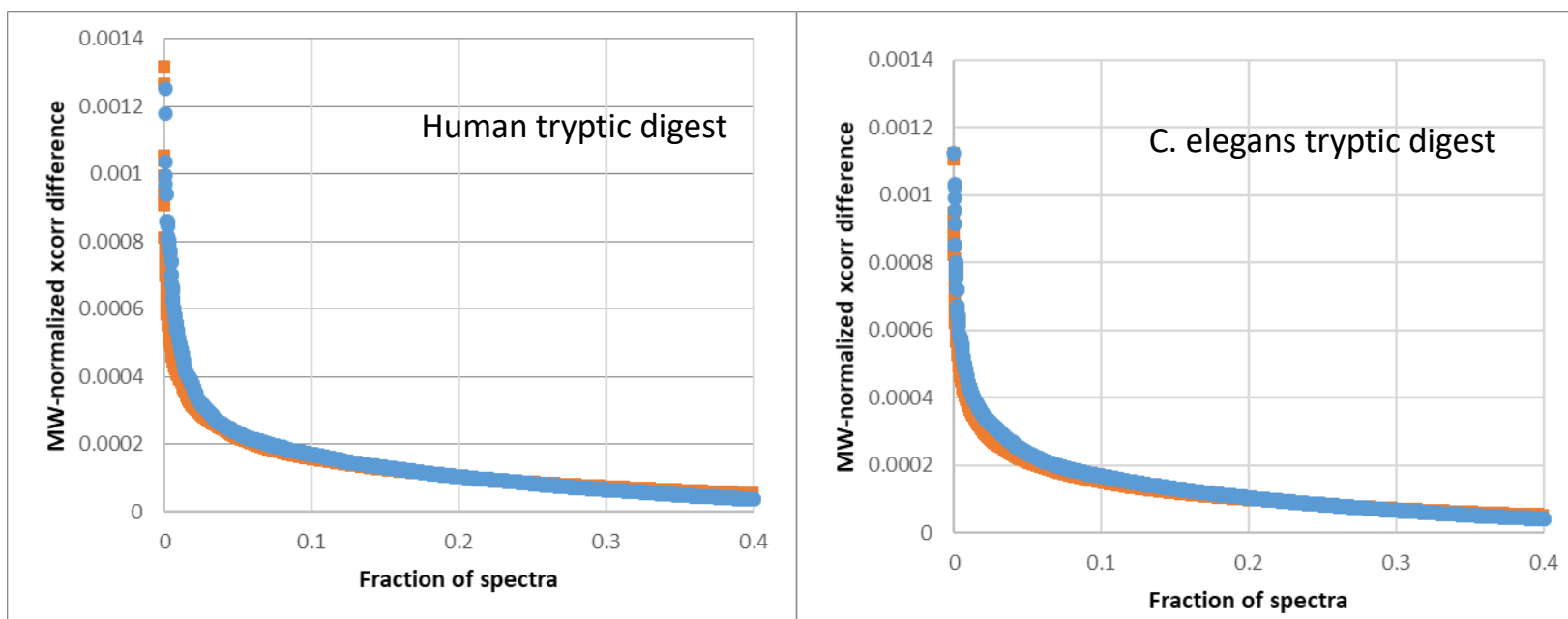
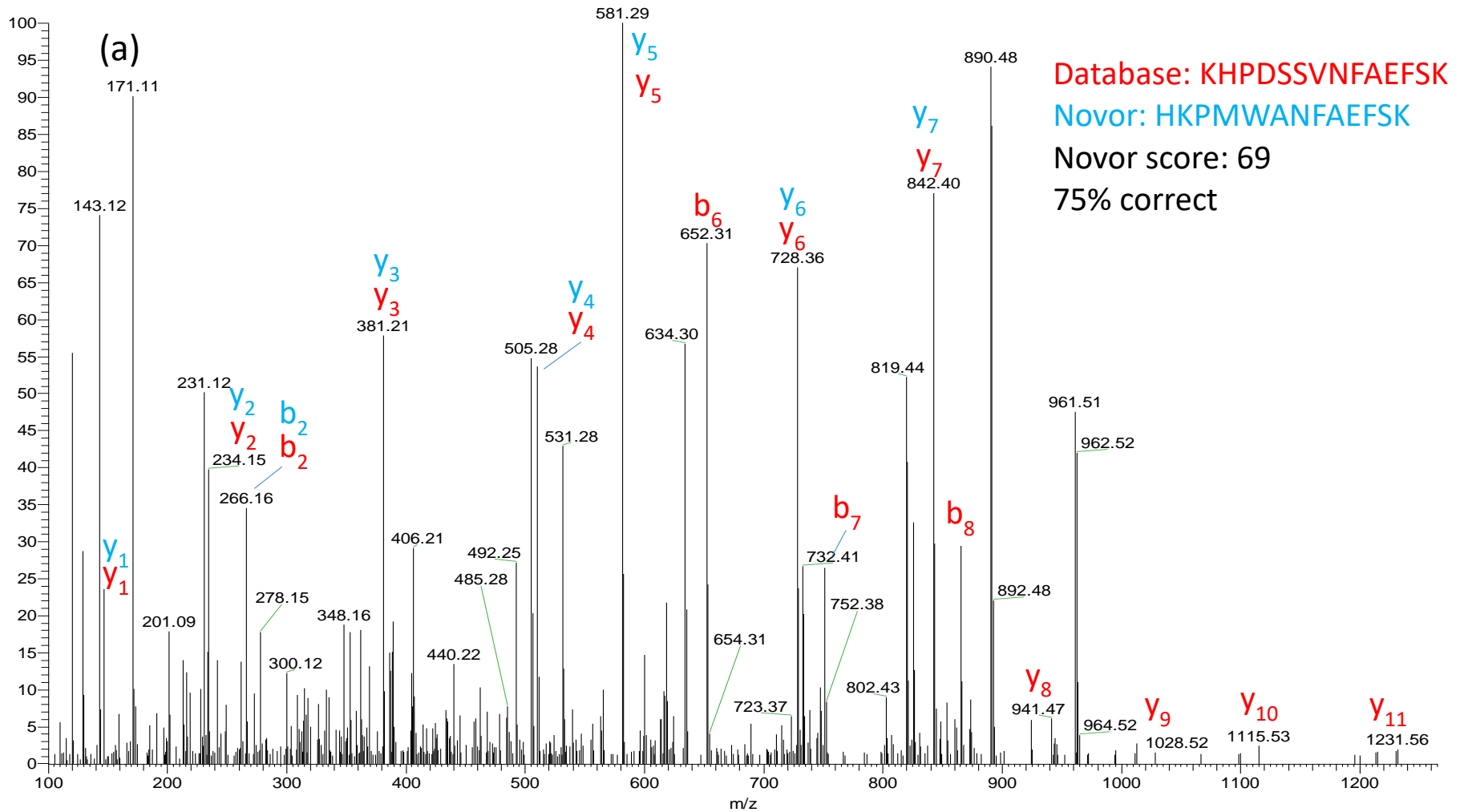
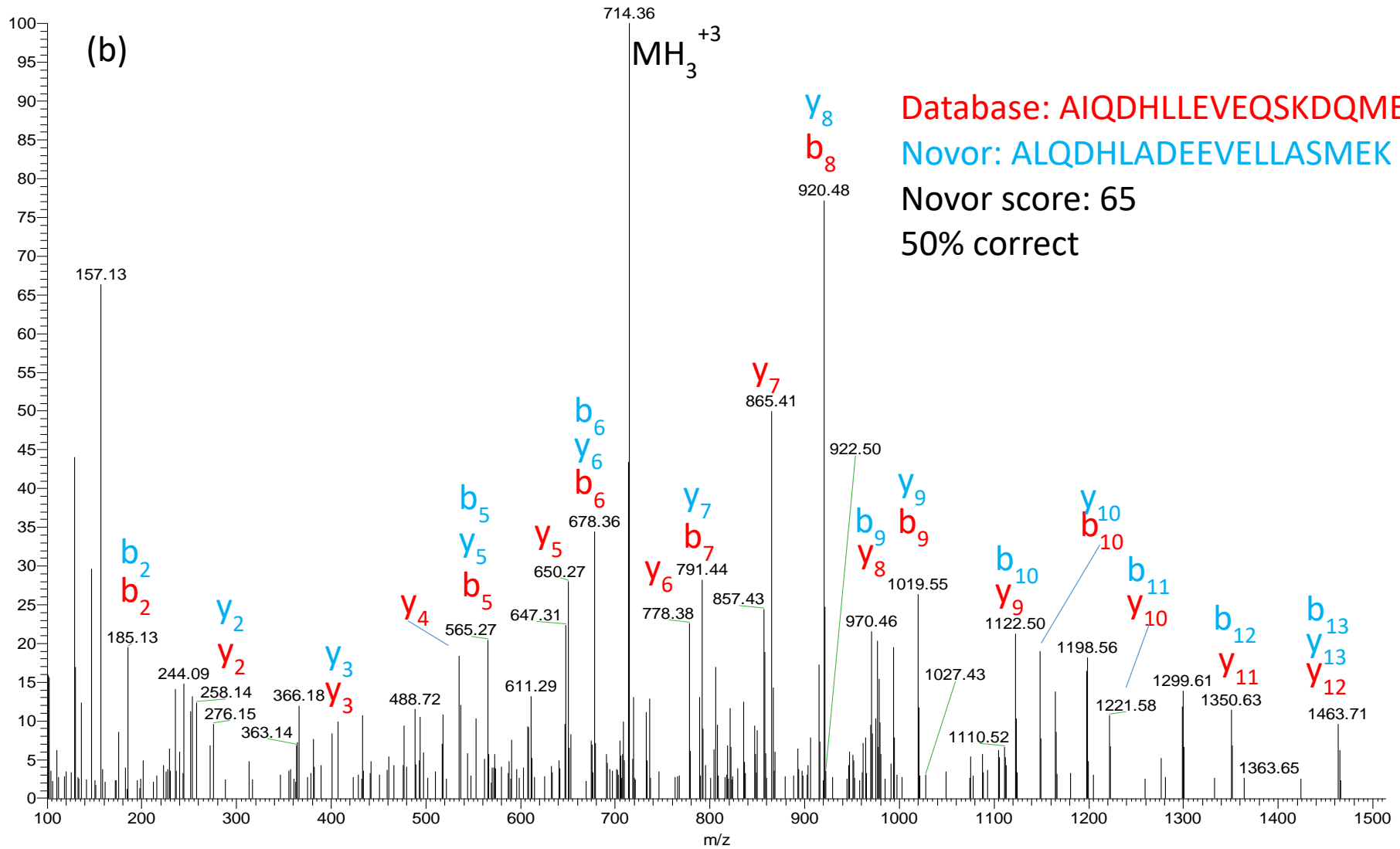


Figure S2: MS/MS spectra for the alignment examples in Fig. 1(b-d). The red labeling indicates fragment ion assignments for the database derived sequence, and the blue labeling shows the assignments for the *de novo* sequence. Most of the unlabeled fragments are due to co-isolation and co-fragmentation of other peptides. Shown are MS/MS spectra of MH_3^{+3} at m/z 531.6 (a), MH_3^{+3} at m/z 714.4 (b), and MH_2^{+2} at m/z 899.4 (c).





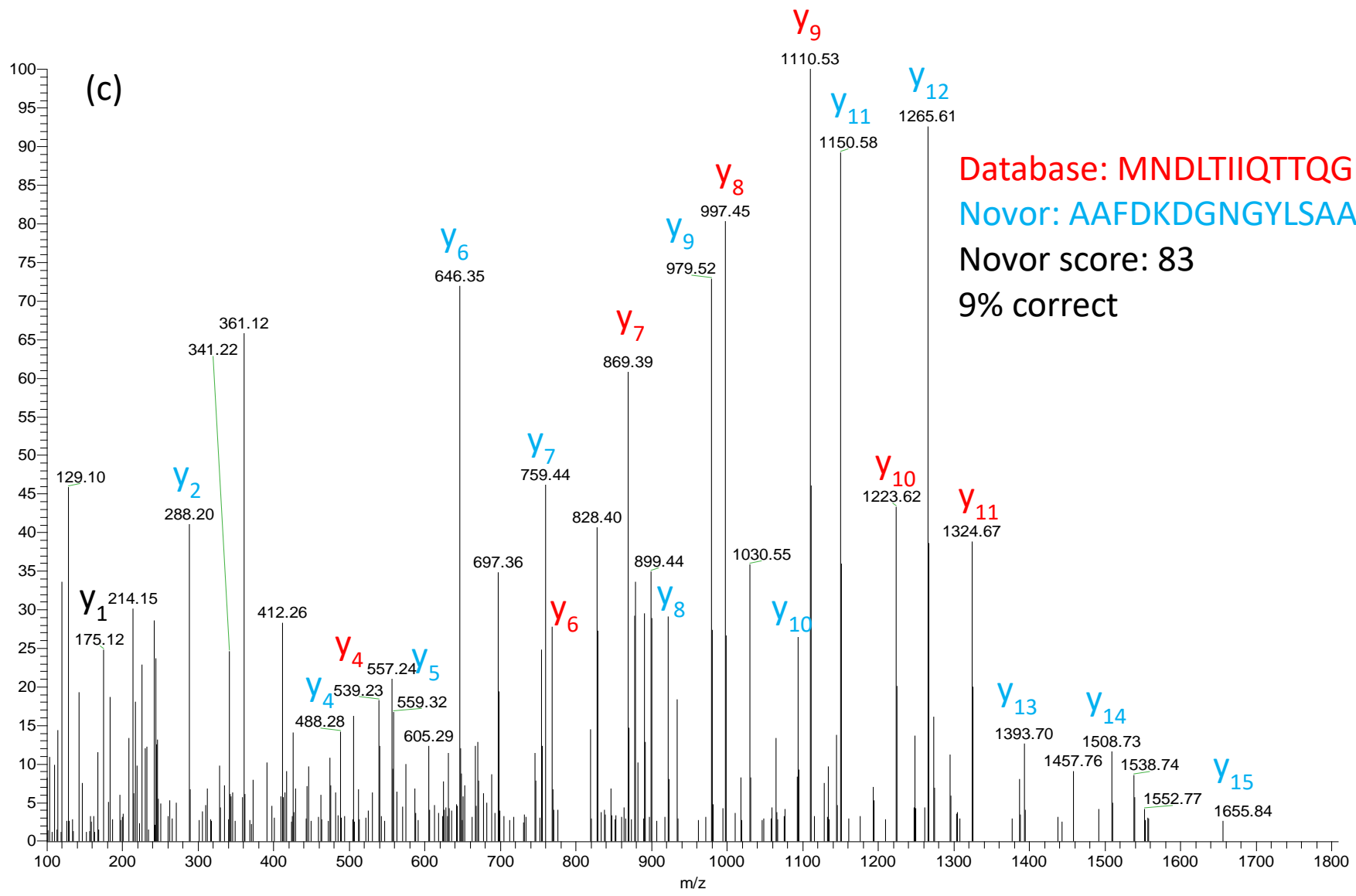


Figure S3: Searching LC-MS/MS data from *C. elegans* tryptic peptides against various FASTA files from different members of the Nematoda phylum. Using a PeptideProphet FDR of 0.01 and maximum Comet E-value of 0.01, the fraction of unique peptides that best matched to FASTA file sequences are shown.

